This article has been accepted for publication in IEEE Access. This is the author's version which has not been fully edited and content may change prior to final publication. Citation information: DOI 10.1109/ACCESS.2023.3325193

IEEE Access
Multidisciplinary | Rapid Review | Open Access Journal

Date of publication xxxx 00, 0000, date of current version xxxx 00, 0000.

*Digital Object Identifier 10.1109/ACCESS.2022.Doi Number*

# Highly Efficient Circularly Polarized Radial Line Slot Array Antenna Using Non-Uniform Slot Density for 5G Communication System

**ONUR CUMURCU[1,2], HAMID TORPI [2], and ALPER CALISKAN[2]**

[1]Informatics and Information Security Research Center (BİLGEM), TÜBİTAK, 41470 Kocaeli, TÜRKİYE
[2]Department of Electronics and Communications Engineering, Yıldız Technical University, 34220 İstanbul, TÜRKİYE

Corresponding author: Onur CUMURCU (e-mail: onur.cumurcu@tubitak.gov.tr).

**ABSTRACT** Radial Line Slot Array (RLSA) antennas have appealing features including high gain and high efficiency combined with a low profile. Especially by highlighting their structural simplicity, RLSA antennas can be good competitors to reflector antennas if the efficiency parameters are improved. In this article, a novel approach is presented to improve the aperture efficiency of RLSAs, with a significant increase of around 10% being achieved. The core principle of this method is the use of non-uniform slot density on the RLSA antenna rings, in addition to non-uniform slot length. RLSA antennas consist of many spiral rings and slots are placed on these rings. With the help of new the concept, slot density has been increased especially on the outer spiral lines, and thus significant improvement has been achieved in both aperture efficiency and return loss. In order to verify the concept, a prototype antenna was fabricated at 26 GHz. The measured results of the prototype antenna show an excellent aperture efficiency of 45%, peak gain of 30.3 dB, and axial ratio of less than 3 dB at operating the frequency band. Also, the antenna reflection coefficient value is less than -10 dB between 24.75 GHz and 27.5 GHz and side lobe levels are below 18 dB, which indicate good pattern characteristic.

**INDEX TERMS** aperture efficiency, high gain, microwave link, radial line slot array, side lobe, 5G.

## I. INTRODUCTION

The increasing interest in complex demanding services (such as high-quality video streaming) and insufficient network capabilities has led to significant research in the fifth generation of wireless standards (5G) [1], [2]. High data rate, ultra-low latency, faster connectivity, and high reliability through the communication channel are the main requirements for the 5G [3]-[5]. These characteristics of the 5G system and some challenges such as the lack of ability to penetrate urban infrastructure require implementing a complicated network in the millimeter wave frequency range. To overcome some obstacles and maintain the quality of services, ultra dense cells with smaller coverage areas can be used. The ultra-dense cells of 5G networks need to handle hundreds of gigabits of traffic from the core network through the backhaul and current cellular system technology. A low-profile and low-cost high-gain antenna technology with directed beam and low-side lobes is essential to realize a dense, robust wireless backhaul. Considering the technical and physical properties of RLSA antennas, it can be a good candidate for use in wireless backhaul. Actually, wireless backhaul provides flexibility and easy installation for 5G base stations, as well as with the use of RLSA antennas wireless backhaul can become more flexible and cost effective.

Parabolic reflector antennas are widely used in microwave links due to the fact that they can provide high directional characteristics [6]. However, such antennas have significant side lobes, especially the nearby sidelobes which are considered a subject interference [7]. Also, the large volume of reflector antennas makes them useless for denser 5G backhaul networks. Radial line slot array antennas (RLSA) on the other hand, have the advantage of low profile, structural simplicity, high gain, and high efficiencies [8].

The RLSA antennas are parallel plate waveguide antennas with a large array of radiating slots strategically cut into the top plate. The use of annular slot radiating elements in



This work is licensed under a Creative Commons Attribution-NonCommercial-NoDerivatives 4.0 License. For more information, see https://creativecommons.org/licenses/by-nc-nd/4

This article has been accepted for publication in IEEE Access. This is the author's version which has not been fully edited and
content may change prior to final publication. Citation information: DOI 10.1109/ACCESS.2023.3325193



planar radial waveguide design was first demonstrated by Goebels and Kelly [9]. Later, Ando and Goto introduced RLSA antennas in the 1980s for direct broadcast satellite services at 12 GHz by improving Goebels and Kelly's works [10]-[12]. Since then, several investigations have been carried out to develop the performance of RLSA antennas. In recent years, some studies, especially targeting low-cost and simple structures, operating at millimeter wave frequency have used printed circuit board (PCB) technology in antenna designs [13]. Some of these researches focused on increasing bandwidth and reducing sidelobe levels [14]-[16]. Highly efficient RLSA antenna studies which consist of two parallel metal plates have also been published to show some electrical parameters like aperture efficiency, directivity, etc. [17], [18]. The RLSA antennas have been used in various applications such as satellite communications, wireless local area networks, high power microwave applications, direct broadcasting satellite, systems and space applications so on [19]-[21].

RLSAs can be designed for both linear polarization (LP) and circular polarization (CP) depending on the orientation of the slots on the top plate. These antennas can also be configured as single or double layer. In double-layered RLSAs, three parallel conducting plates are separated to form a two-fold radial waveguide cavity, and the slots are excited by an inward travelling transverse electromagnetic (TEM) wave while, in single-layered RLSAs, they consist of two parallel plates and slots are excited by a radially outward travelling transverse electromagnetic (TEM) wave [22]. When it comes to manufacturing and performance, there is a trade-off. A single-layered RLSA is easier to manufacture however, a double-layered RLSA can be designed to achieve a higher aperture efficiency [16].

Modern communication systems require a highly efficient antenna system in order to meet the demanding requirements of wireless communication. An efficient antenna system does not only mean the best antenna parameters such as high directivity, wideband, low side lobe, etc. but also low cost and easy installation. Because of their low profile and structural simplicity, RLSA antennas can be easily installed in roof-top on mobile vehicles. In addition, these antennas are not subject to rain or snow build up which can degrade performance due to planar surface, so weather conditions do not interrupt communication.

The aim of this paper is to develop a low-cost, high gain CP RLSA antenna for 5G applications. To achieve high directive RLSA antennas at the 5G frequency range, slot configuration on the top plate must be done appropriately. Some articles on high gain RLSA control the aperture field distribution with slot coupling [23]-[25]. By varying the slot lengths through the antenna, the energy coupled from the inner cavity to the radiating plate can be controlled. In this paper, the slot lengths are varied to obtain a uniform phase distribution, also a method is presented to improve antenna gain and the method is validated by simulation and measurement results of the prototype antenna. With the proposed method, both lengths and slot densities are varied, and thus non-uniform slot distributions are obtained. By increasing slot densities away from the antenna center, incident power from the feeder is used more efficiently and the antenna's overall performance is enhanced.

The rest of this article is organized as follows. Section II describes the RLSA antenna configuration and gives fundamental equations for the design process. In Section III, radiator placement on the metal sheet is theoretically studied. The proposed design concept is explained by comparing classical approaches and its performance is demonstrated with full wave simulations in Section IV. Prototype antenna measurement results are reported in Section V. Finally, the main conclusion of this work is drawn in Section VI.

## II. ANTENNA CONFIGURATION

In order to grasp the proposed high gain antenna, it is crucial to understand the basic configuration of the classical RLSA with a uniform TEM waveguide. The structure of a conventional RLSA antenna is shown in Fig. 1. It has a radial waveguide formed between two metal plates. The top metal plate has a ring of radiating slots strategically placed to control gain and polarization. The metal plate at the bottom acts as a ground plane and there is an aperture in the center for the feeding probe. The two metal plates are separated by a cavity. Depending on the application, that cavity can be filled with a dielectric material to suppress grating lobes, but this brings some difficulties in the manufacturing process. In conjunction with radiating slots and ground plate, the cavity acts as a circular waveguide guiding the signal from the feeder to propagate in a radial direction. For easy production and low-cost RLSA antenna, in this paper the cavity is filled with air, and grating lobes do not appear thanks to ground plane design. RLSA antenna is fed through a 50 Ω coaxial probe at the center of the ground plane. The top end of the probe is terminated with a disc head for impedance matching and efficient excitation of the radial waveguide.

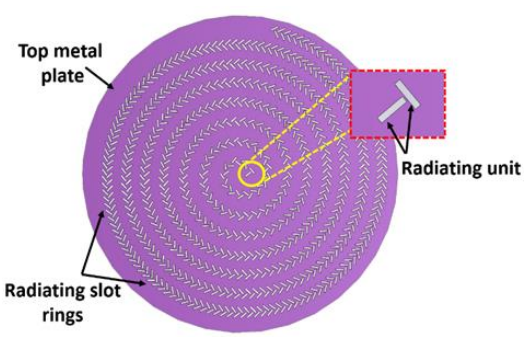


**FIGURE 1. CP RLSA antenna configuration.**



This work is licensed under a Creative Commons Attribution-NonCommercial-NoDerivatives 4.0 License. For more information, see https://creativecommons.org/licenses/by-nc-nd/4

This article has been accepted for publication in IEEE Access. This is the author's version which has not been fully edited and
content may change prior to final publication. Citation information: DOI 10.1109/ACCESS.2023.3325193



### A. THEORETICAL PRINCIPLE OF WAVEGUIDE CAVITY

The cross section of the RLSA is shown in Fig. 2. The cavity is filled with air and operates symmetrical transverse electromagnetic wave mode. Electromagnetic power is fed through a coaxial probe at the center of the ground plane and radially outward travelling wave mode is generated. Thanks to the disc head at the end of coaxial probe, power is converted from coaxial mode into the waveguide mode. Radial currents travelling outwardly within the waveguide radiate from slots that cut on the top plate. The height of the waveguide (h) must be less than half of the free space wavelength ($\lambda_0$) to prevent propagation of any higher order modes. If waveguide height is less than half of the free space wavelength ($h < \lambda_0$), the only possible symmetrical mode is the TEM mode whose magnetic field is given by [10]:

$$H_\varphi(\rho) = H_1^{(2)}(k\rho) - \Gamma \frac{H_1^{(2)}(k\rho_{max})}{H_1^{(1)}(k\rho_{max})} H_1^{(2)}(k\rho) \quad (1)$$

$\rho$ = Radial position.
$k = 2\pi / \lambda_0$ wave number in the radial waveguide.
$\Gamma$ = Reflection coefficient.
$H_1^{(1)}(k\rho)$ = Henkel function of first kind of order.
$H_1^{(2)}(k\rho)$ = Henkel function of second kind of order.

In equation (1), the first term shows the outward travelling wave excited by the coaxial probe, while the second term represents the inward travelling waves. The reflection coefficient is very small for large aperture antennas due to a considerably low level of power at the end of the antenna. Therefore, the reflection coefficient is negligible, and (1) can be rewritten as follows:

$$H_\varphi(\rho) \approx H_1^{(2)}(k\rho) \quad (2)$$

The theoretical slot design is similar to that proposed in [26]. As shown in Fig. 2, slot geometry in this article is placed on the single-layered cavity. Radiating units are defined as an adjacent slot pair lying along the $\varphi$ direction. When the cavity height is chosen correctly ($h < \lambda_0$), the inner field behaves as a TEM wave whose variation with cavity radius is approximated by [27]

$$F(\rho) \propto e^{-jk\rho} \quad (3)$$

where $k$ is the wave number in the radial waveguide. Waveguide magnetic field has one component in $\varphi$ direction, so the surface current is the radial current, proportional to $H_\varphi$. For a given slot, the coupled field correlates directly with the slot orientation factor as given by [27]

$$F = e^{-jk\rho} \sin\theta \quad (4)$$

where $\theta$ is the angle between slot and current flow line.

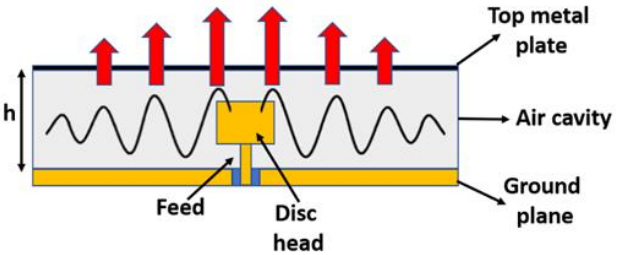


**FIGURE 2.** Cross section view of the CP RLSA antenna.

### B. RADIATING UNIT DESIGN

The top metal plate, which can also be defined as a radiating plate, has a lot of radiating units. Unit radiators consist of two slots that are spatially orthogonal and thus radiate two orthogonal electric field components with equal magnitude [28]. The center of the antenna is indicated by the point O, which is also the location of the feeder, as shown in Fig. 3. It can be seen that the slots which constitute the radiating units are at a certain distance from the center, represented as $\rho_1$ and $\rho_2$ respectively. To obtain a high- performance antenna, radiating units are located according to the current flow line. The ideal current flow line is depicted in Fig. 3, and two orthogonal slots make angles of $\theta_1$ and $\theta_2$ with their current flow line.

The orientation of the slots on the radiating plate determines the polarization of the antenna. To obtain CP RLSA, two slots are placed orthogonally in the unit radiator and radiate with the same magnitude. Also, the difference in radial distance of two slot centers is set to a quarter of the free space wavelength in order to create a 90° phase shift [24], [25]. When slots are arranged according to the procedure defined above, two orthogonal electric field components with equal magnitude are obtained.

For circular polarization, the difference between two slots in the same unit radiator is equal to a quarter of the free space wavelength as follows [27]

$$\rho_1 - \rho_2 = \frac{\lambda_0}{4} \quad (5)$$

When placing the radiating units, the slots should not overlap each other. To avoid overlapping, the first and second slots in a radiating unit must be located on different radial lines by keeping $\lambda_0/4$ spacing between them. If the second slot is shifted in $\varphi$ direction and positioned $\rho_2$ from the origin, it will locate a different current flow line, and also overlap will not appear. Equations (6) and (7) can be used for second slot placement [23].

$$\theta = \tan^{-1} \frac{\frac{\lambda_0}{4\sqrt{2}}}{\rho_1 + \frac{\lambda_0}{4\sqrt{2}}} \quad (6)$$

$$\rho_2 = \frac{\frac{\lambda_0}{4\sqrt{2}}}{\sin\theta} \quad (7)$$



This work is licensed under a Creative Commons Attribution-NonCommercial-NoDerivatives 4.0 License. For more information, see https://creativecommons.org/licenses/by-nc-nd/4

This article has been accepted for publication in IEEE Access. This is the author's version which has not been fully edited and content may change prior to final publication. Citation information: DOI 10.1109/ACCESS.2023.3325193



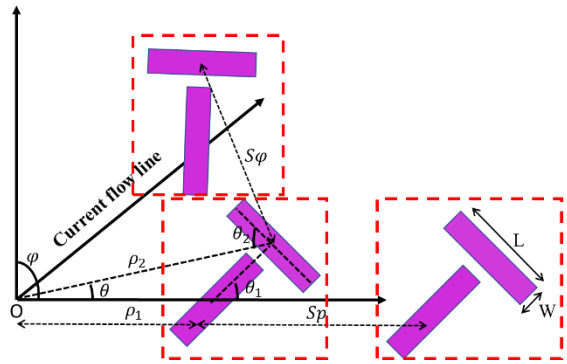


**FIGURE 3.** **Arrangement of slot pair.**

### C. FEED STRUCTURE

The RLSA antenna is excited at the center of the ground plane by using commercially available SMA connectors. The maximum power transfer from the SMA to the RLSA antenna depends on the feed structure. For this reason, the SMA connector must be optimized by adding a disc head at the top end.

Fig. 4 shows in detail the parameters of the optimized feed structure and also parameters of the feeder part of the designed antennas are presented in Table I.

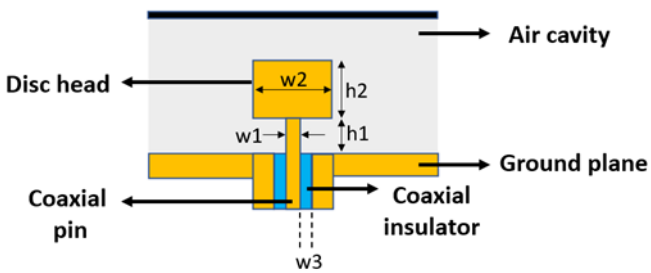


**FIGURE 4.** **Cross-sectional view of the feeder**

TABLE I
DESIGN PARAMETERS OF FEEDER

| Parameter | Value (mm) |
|---|---|
| Width of coaxial pin (w1) | 1.3 |
| Width of disc head (w2) | 2.8 |
| Width of coaxial insulator (w3) | 1.4 |
| Air gap between disc head and ground plane (h1) | 1.6 |
| Height of disc head (h2) | 2.4 |

## III. DESIGN METHOD

### A. SLOT ARRANGEMENT

After designing the radiating unit, the next step is to create a large array on the top plate. By using (5), (6) and (7), the radiating units are cut on the top, and form a spiral ring along the $\varphi$ direction, as shown in Fig. 5. There are some significant physical parameters about RLSA antenna design and these parameters directly affect antenna performance. The center-to-center spacing between two radiating units in the radial and spiral directions are denoted by $S_p$ and $S_\varphi$ respectively as shown in Fig. 6 [23], [27]. $S_\varphi$ can be chosen arbitrarily based on the slot density on the top plate, but $S_p$ is kept equal to free space wavelength ($\lambda_0$). For best results, these parameters, especially $S_\varphi$, can be optimized away from the center.

Visual Basic Macro (VBA) can be used to design the slot layout on the top plate. By utilizing VBA, performance enhancements can be made quickly. To create a large slot array, unit radiators should be placed at a certain distance from the center and form rings [23], [27]. Equation (8) and (9) shows an approximate function for defining unit radiator distance from the center. Creating a loop in the VBA, placement of slots can be done quickly with some physical antenna parameters such as $S_p$, and $S_\varphi$.

$$\rho_n = \rho_1 + i\left(\frac{\lambda_0}{sn}\right) + (rn-1)\lambda_0 \tag{8}$$

$$\varphi_n = \cos^{-1}\frac{S_\varphi{}^2 - \rho_{n-1}{}^2 - \rho_n{}^2}{2(\rho_{n-1})(\rho_n)} \tag{9}$$

$\rho_1$: First unit radiator distance from the center.
$\rho_n$: n. unit radiator distance from the center on the rn. ring.
$i$: Active unit radiator number on the rn. ring.
$\lambda_0$: Free space wavelength.
$sn$: Slot number belog to rn. ring.
$rn$: Ring number.
$\varphi_n$: n. slot phi angle on the rn. ring.
$S_\varphi$: The center to center spacing between two radiating unit in the spiral direction.

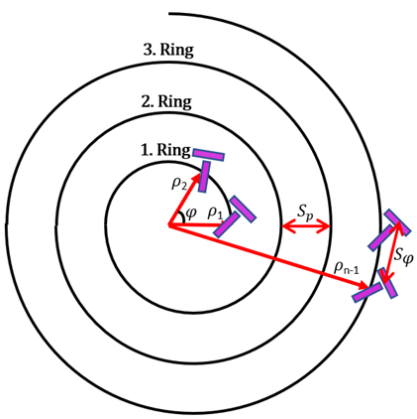


**FIGURE 5.** **Spiral line configuration on the top plate of the CP RLSA antenna.**



This work is licensed under a Creative Commons Attribution-NonCommercial-NoDerivatives 4.0 License. For more information, see https://creativecommons.org/licenses/by-nc-nd/4

This article has been accepted for publication in IEEE Access. This is the author's version which has not been fully edited and
content may change prior to final publication. Citation information: DOI 10.1109/ACCESS.2023.3325193



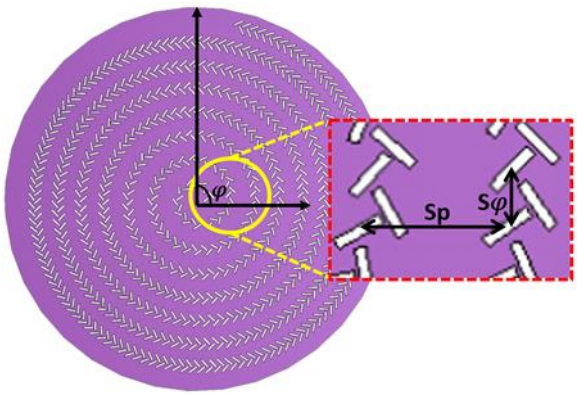


**FIGURE 6.** **Slot arrangement on the top plate of the CP RLSA antenna**

### *B. SLOT DISTRIBUTION ON THE TOP SURFACE*

When designing an RLSA antenna, the unit radiator should be strategically cut on the top metal plate. In terms of far field pattern quality and boresight gain, the power radiated from the slots on the top surface must be controlled to achieve uniform aperture illumination. The amount of power radiated from slots depends on some parameters such as slot density and number of slots. Therefore, by adjusting these parameters, slot excitation and illumination can be controlled.

Slot coupling analysis is critical for aperture illumination. This analysis has been done by varying the slot length from center to edge of the antenna so, the slot density can be kept constant on the top plate. If all slot length through rings has the same value, the power density of the outward travelling wave will be decreased. The slot length is varied to the following equation.

$$L_{slot}=\&+(\rho*a) \tag{10}$$

$\&$: Constant value
$\rho$: Radial distance
$a$: Coupling coefficient

The product $(\rho*a)$ is defined as the coupling factor in (10). The coupling factor increases with the radial distance and so larger slots are formed. The coupling energy from the travelling wave into the radiating slots can be controlled by varying the slot length [23], [24].

The power denoted $P$ comes from the center of the antenna and flows towards the edge of the antenna, as shown in Fig. 7. When the incident power from the feeder is cut by slots, a certain amount of power radiates through the slots and the rest flows to the antenna edge. As the travelling wave radiates through the slots, the total power inside the cavity decreases. Equation (11) shows the remaining power after the travelling wave has radiated from the slots [29].

$$P_r = P(1-a)^n \tag{11}$$

$P_r$: Remaining power
$n$: Ring number
$P$: Maximum power

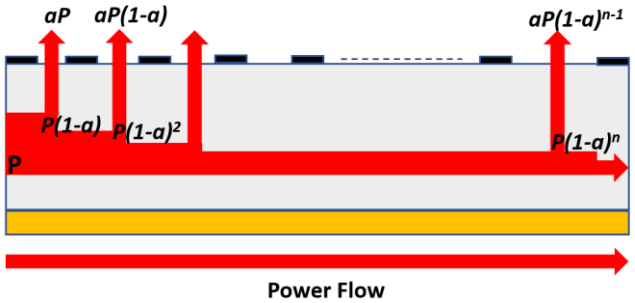


**FIGURE 7.** **Power flow inside air cavity of the CP RLSA antenna.**

The amount of remaining power at the end of the antenna depends on the number of rings, so if the antenna is not large enough, the remaining power at the end will be high. Part of this remaining power reflects back to the feeder so the reflection coefficient of the antenna deteriorates.

## IV. INVESTIGATION ON NONUNIFORM SLOT DISTRIBUTION

Slot distribution has so strong effect on the performance of RLSA antennas. In the previous section, this effect is briefly explained with figures and equations. In particular, slot length variation on the surface of the top plate is a useful technique to improve RLSA antenna performance, and some articles using this technique have been published in recent years. However, in this article, the non-uniform slot distribution approach has been further developed by varying the slot densities in accordance with the number of rings. Varying the slot density in addition to the classical approach of adjusting only the slot lengths from center to antenna edge improves RLSA antenna efficiency.

In order to verify the new concept, a CP RLSA antenna operating at 25-27.5 GHz was designed. The diameter of this antenna is 180 mm and it consists of 7 spiral rings. The slot orientation on the top plate and ground plate was created according to previous sections and reported articles [23].

First of all, by keeping the $S_\varphi$ constant, we observed the effect of slot length ($S_l$) on the antenna performance. As the slot length decreases from the half wavelength, the antenna directivity and aperture efficiency improve, but on the other hand, the return loss value increases. This is because the amount of energy at the antenna edge is too high due to the small slot length. As a result, some of energy reflects back from the antenna edge, causing the reflection coefficient value to remain above -10 dB.

Secondly, the slot length is increased from the center to the antenna edge according to (10). When the slot length varies as a function of radius, a positive effect on both gain and aperture efficiency was observed.

Fig. 8 and Fig. 9 show broadside directivity and reflection coefficient variation according to the coupling coefficient. When considering important antenna parameters like directivity, matching, side lobe level, etc., coupling coefficient was chosen as 0.008 mm.



This work is licensed under a Creative Commons Attribution-NonCommercial-NoDerivatives 4.0 License. For more information, see https://creativecommons.org/licenses/by-nc-nd/4

This article has been accepted for publication in IEEE Access. This is the author's version which has not been fully edited and
content may change prior to final publication. Citation information: DOI 10.1109/ACCESS.2023.3325193



The far field radiation patterns and reflection coefficient of the antennas with different slot lengths are shown in Fig. 10 and Fig. 11 respectively.

Table II lists the peak directivity, side lobe level (SLL), and $S_{11}$ value at 26 GHz for certain values of $S_l$, and it can be seen that slot length is an important parameter to achieve high performance RLSA antenna. In particular, the sixth row in Table II shows a perfect improvement in antenna performance. The $L_{slot}$ value starts from 4.23 mm at ring 1 and ends with 4.76 mm at ring 7. While determining these values, (10) was used and the parameter & was kept constant at 4.2 mm, however coupling coefficient ($a$) was varied between 0.002 and 0.012 to achieve high aperture efficiency.

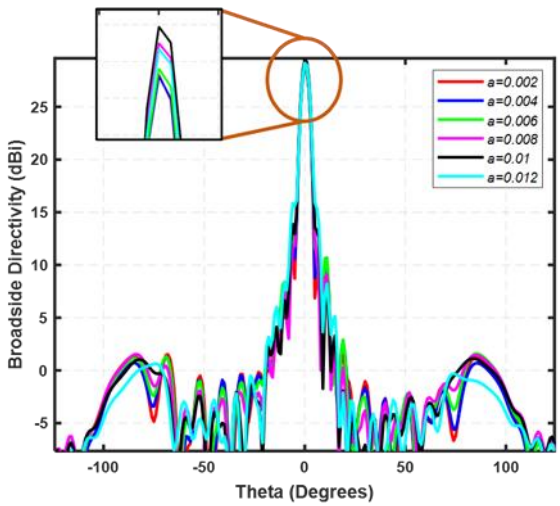


**FIGURE 8.** **Broadside directivity for different coupling coefficients at 26 GHz**

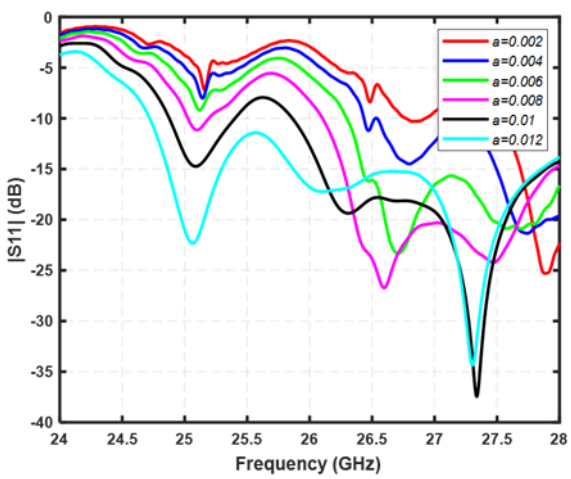


**FIGURE 9.** **Reflection coefficient magnitude $|S_{11}|$ for different coupling coefficients.**

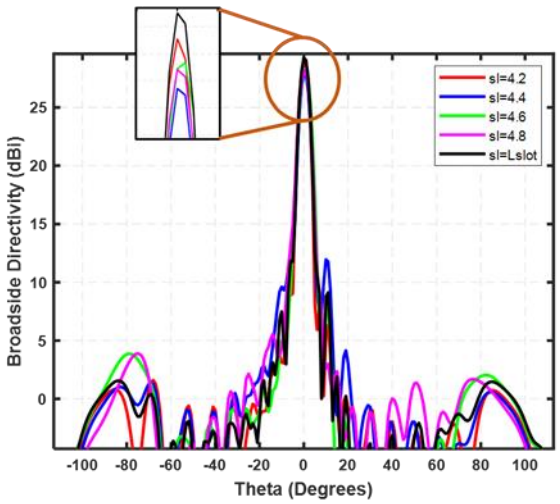


**FIGURE 10.** **Broadside directivity for different slot lengths at 26 GHz**

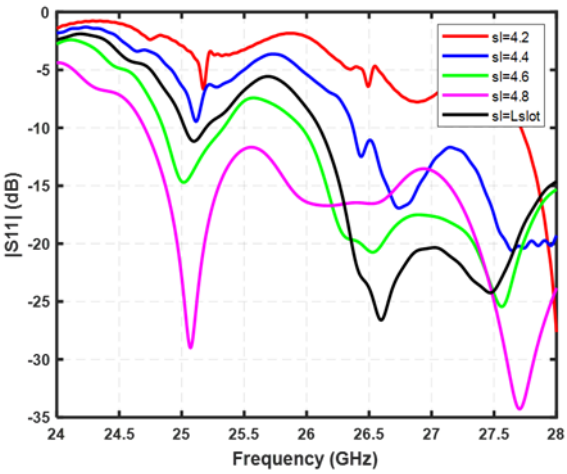


**FIGURE 11.** **Reflection coefficient magnitude $|S_{11}|$ for different slot lengths**

TABLE II
ANTENNA PERFORMANCE FOR DIFFERENT SLOT LENGTH AT 26 GHZ

| $S_l$ | $S\varphi$ | Directivity | SLL | $S_{11}$ | Aperture Efficiency |
|---|---|---|---|---|---|
| mm | mm | dBi | dB | dB | % |
| 4.2 | 5 | 28.8 | -19.5 | -2.13 | 31.6 |
| 4.4 | 5 | 27.9 | -15.9 | -5.4 | 25.6 |
| 4.6 | 5 | 28.3 | -20.6 | -10.6 | 28.1 |
| 4.8 | 5 | 28.2 | -22.6 | -16.4 | 27.5 |
| $L_{slot}$ | 5 | 29.2 | -17.4 | -8.3 | 34.6 |

In this article, the effect of changing slot length on the antenna performance has been observed in the studies carried out so far, and the results are shown with figures and tables. From Table II, it can be seen that while the aperture efficiency



This work is licensed under a Creative Commons Attribution-NonCommercial-NoDerivatives 4.0 License. For more information, see https://creativecommons.org/licenses/by-nc-nd/4

This article has been accepted for publication in IEEE Access. This is the author's version which has not been fully edited and
content may change prior to final publication. Citation information: DOI 10.1109/ACCESS.2023.3325193



improves, the $S_{11}$ deteriorates. When (10) is used for determining slot length, the $S_{11}$ value is slightly improved but it is not sufficient.

In this study, we recommended a new concept to achieve high aperture efficiency and low side lobe levels. The concept involves a non-uniform slot density on the radiating plate. Our aim with the new concept is to increase the radiated power from the slots placed on the top plate. By increasing both the slot length and the slot density towards to antenna end, more electromagnetic waves in the air cavity can radiate and a high performance RLSA antenna can be obtained.

In order to vary slot density for each ring on the top plate, center-to-center spacing between two radiating units in a spiral direction, which is denoted by $S_\varphi$ can be arranged. However, when making this arrangement the overlapping of the unit radiator with each other should be avoided. In addition to overlapping, the production process must be considered. If $S_\varphi$ is too small, laser cutting tolerance cannot meet that small distance between two radiating units so faulty production may occur.

The parameters given in Table III are used to design a new concept antenna. As can be seen from Table III, both $S_l$ and $S_\varphi$ can be varied depending on the ring number and radial distance from the center.

TABLE III
SIGNIFICANT PHYSICAL PARAMETERS OF THE NEW CONCEPT ANTENNA

| Ring Number | $S_l$ (mm) | $S_\varphi$ (mm) | $S_p$ (mm) |
|---|---|---|---|
| 1 | 4.23 | 4.7 | 11 |
| 2 | 4.32 | 4.7 | 11 |
| 3 | 4.41 | 4.45 | 11 |
| 4 | 4.5 | 4.1 | 11 |
| 5 | 4.58 | 4.25 | 11 |
| 6 | 4.67 | 4.1 | 11 |
| 7 | 4.76 | 3.7 | 11 |

The near field propagation of the designed antenna at the operating frequency is given in Fig. 12. The time-varying near field distribution of the Ex component in the cross section of the XZ-plane was taken at the distance of $3\lambda_0$ from the antenna surface. As can be seen from the field distributions the antenna has nearly linear phase fronts at operating frequency.

The broadside directivity and magnitude of the input reflection coefficient of the antenna designed with two concepts are compared in Fig. 13 and Fig. 14. The results detailed in Table IV show that the new concept antenna has an edge on classic RLSA design.

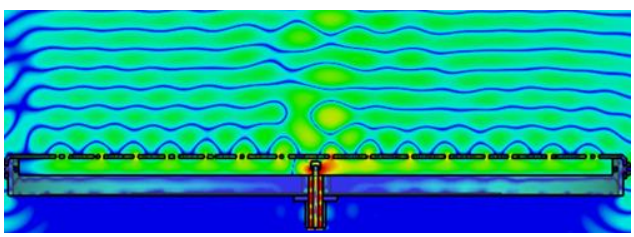

**FIGURE 12. 2-D views of electric near-field aperture distribution at 26 GHz**

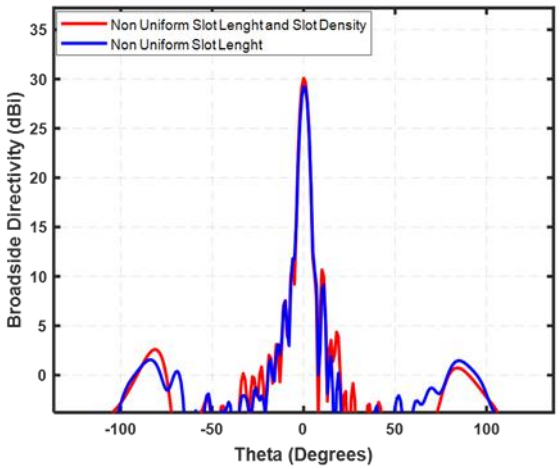


**FIGURE 13. Comparison of the broadside directivity of the RLSAs with new non-uniform concept and classic concept**

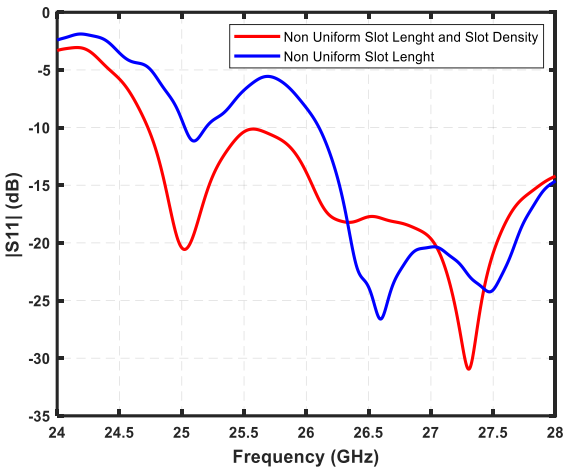


**FIGURE 14. Comparison of reflection coefficient magnitude $|S_{11}|$ of the RLSAs with new non-uniform concept and classic concept**

TABLE IV
COMPARISON OF TWO NON-UNIFORM CONCEPT CP RLSAS

| Works | Directivity | SLL | $S_{11}$ | Aperture Efficiency | Axial Ratio |
|---|---|---|---|---|---|
| | dBi | dB | dB | % | dB |
| Non-Uniform Slot Length | 29.2 | -17.4 | -8.3 | 34.6 | 0.9 |
| Non-Uniform Slot Length and Non-Uniform Slot Density (new concept) | 30.6 | -18.7 | -13.9 | 47.8 | 0.9 |



This work is licensed under a Creative Commons Attribution-NonCommercial-NoDerivatives 4.0 License. For more information, see https://creativecommons.org/licenses/by-nc-nd/4

This article has been accepted for publication in IEEE Access. This is the author's version which has not been fully edited and
content may change prior to final publication. Citation information: DOI 10.1109/ACCESS.2023.3325193



## V. PROTOTYPE AND RESULTS

### A. ANTENNA PROTOTYPE

A prototype antenna was developed to verify the concept of the non-uniform slot density and slot length at the operating frequency of 26 GHz. The parameters of the final design are given in Table V. The slot layout on the top plate, shown in Fig. 15(a), was created using VBA in CST Microwave Studio. The antenna has 7 spiral rings of slots cut on the top plate with a diameter of $15.5\lambda_0$. During the development of the prototype, two different methods were used, respectively laser cutting and water jet cutting. In both methods, slots were cut 1 mm thick of aluminum, but some problems were encountered. The main disadvantage of laser cutting was that the top plate was not flat. This was due to the high heat input of the laser beam when etching the large number of slots in the metal sheet. The negative side of the waterjet cutting process was that the slots were not cut with the same precision as the laser cutting process. Because of its high precision, laser cutting is preferred in this study. To overcome the flatness problem, the top metal plate is screwed to the bottom ground plane with lugs opening from all four corners, as illustrated in Fig. 15(b). In addition, extra support was provided by using aluminum glue on the edges.

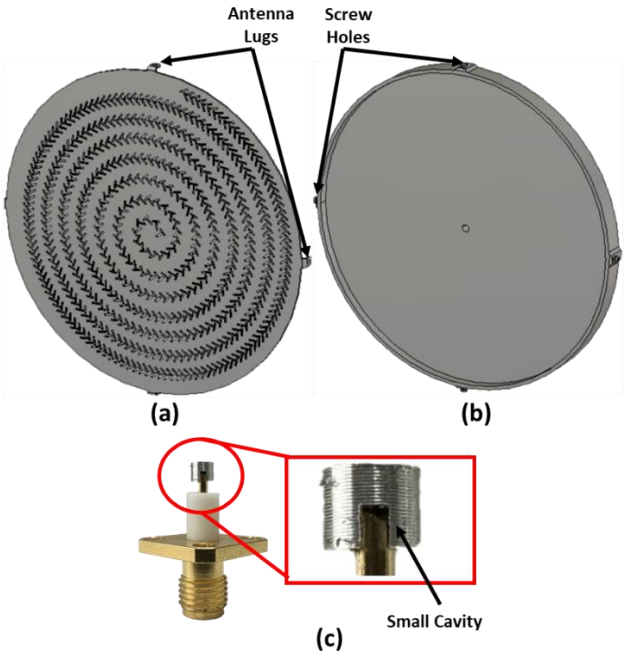


**FIGURE 15.** CP RLSA antenna parts. (a) Radiating top plate with lugs, (b) Ground plate with screw holes, (c) Feeder with disc head

### B. INPUT MATCHING

The magnitude of the input reflection coefficient of the prototype antenna was measured with a vector network analyzer. The feeding probe has a significant effect on the reflection coefficient results. The probe end with a disc-head for matching and efficient power transfer. In addition, a small cavity, shown in Fig. 15(c), was opened on the disc head to be soldered to the inner pin of probe for better transmission and durability. The measured and simulated results are compared in Fig. 16. The measured results show that the reflection coefficient is less than -10 dB at the operating frequency, and they match well with the simulated result. There may be some differences between the simulation and measurement results due to some manufacturing related issues such as laser cutting accuracy and a little deformation on the top plate.

TABLE V
PARAMETERS OF THE NEW CONCEPT ANTENNA

| Parameters | Value |
|---|---|
| Free space wavelength ($\lambda_0$) | 11.5 (mm) |
| Slot lengths ($S_l$) | 4.23-4.76 (mm) |
| Slot depth | 1 (mm) |
| Slot width | 0.88 (mm) |
| Unit radiator spacing along radial directions ($S_\rho$) | 11.5 (mm), $\lambda_0$ |
| Unit radiator spacing along spiral directions ($S_\varphi$) | 4.7-3.7 |
| Number of rings | 7 |
| Aperture diameter | 180 (mm) |
| Air cavity height | 5 (mm) |

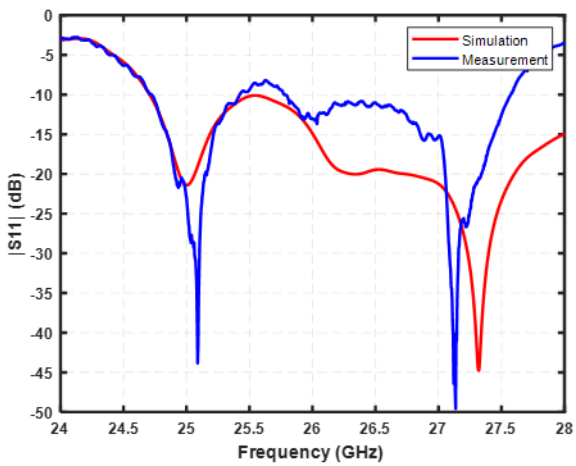


**FIGURE 16.** Reflection coefficient magnitude $|S_{11}|$ of the CP RLSA antenna

### C. RADIATION PATTERN AND AXIAL RATIO

The prototype antenna has a high quality and stable radiation pattern at the operating frequency. The radiation pattern measurements were carried out at Antenna Test and Research Laboratory in TUBITAK, as illustrated in Fig. 17. The simulated and measured radiation patterns in $\varphi=0°$, $\varphi=90°$ are shown in Fig. 18 and Fig. 19. The axial ratio of the simulated and prototype antennas is compared in Fig. 20. It can be seen that axial ratio remains below 3 dB level over the operating frequency band, meeting the circular polarization condition. In addition, 3 dB gain bandwidth of the prototype CP RLSA is depicted in Fig. 21.



This work is licensed under a Creative Commons Attribution-NonCommercial-NoDerivatives 4.0 License. For more information, see https://creativecommons.org/licenses/by-nc-nd/4

This article has been accepted for publication in IEEE Access. This is the author's version which has not been fully edited and content may change prior to final publication. Citation information: DOI 10.1109/ACCESS.2023.3325193



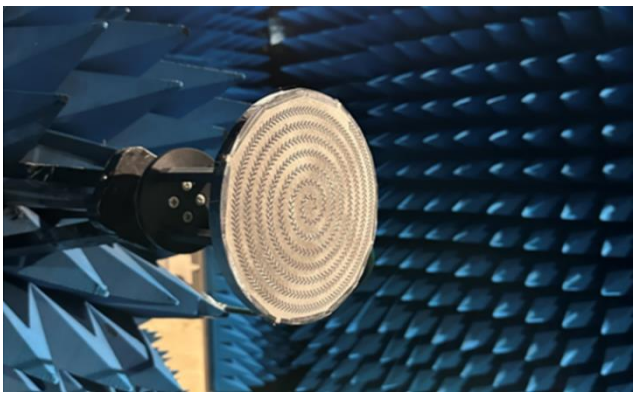

**FIGURE 17.** **Measurement setup of the prototype CP RLSA antenna**

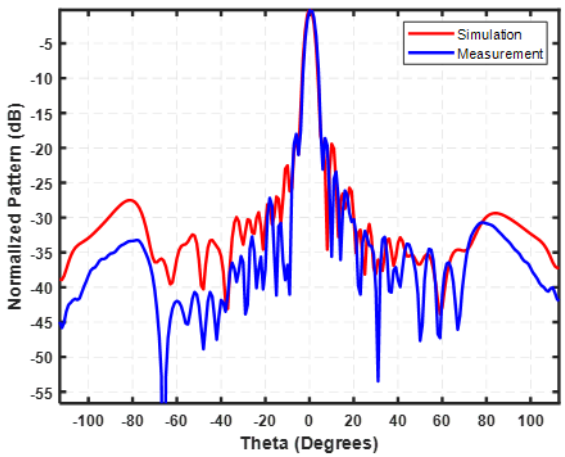


**FIGURE 18.** **Radiation pattern of the prototype CP RLSA antenna on φ=0° plane at 26 GHz**

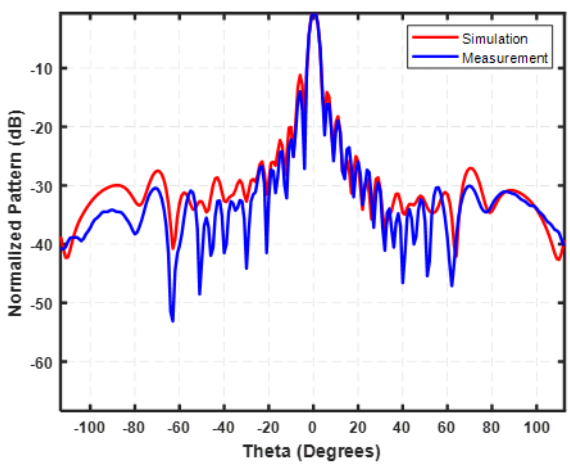


**FIGURE 19.** **Radiation pattern of the prototype CP RLSA antenna on φ=90° plane at 26 GHz.**

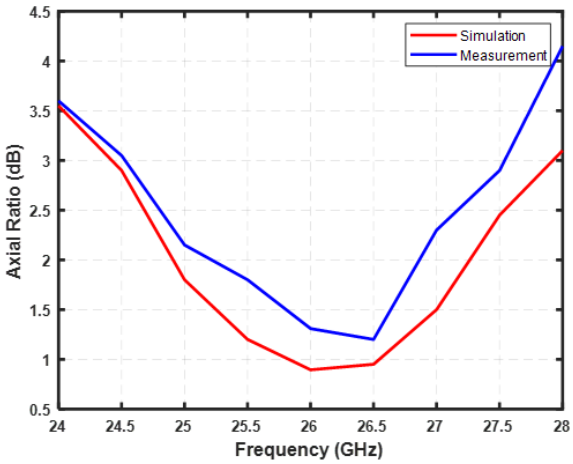


**FIGURE 20.** **Axial ratio of the prototype CP RLSA antenna**

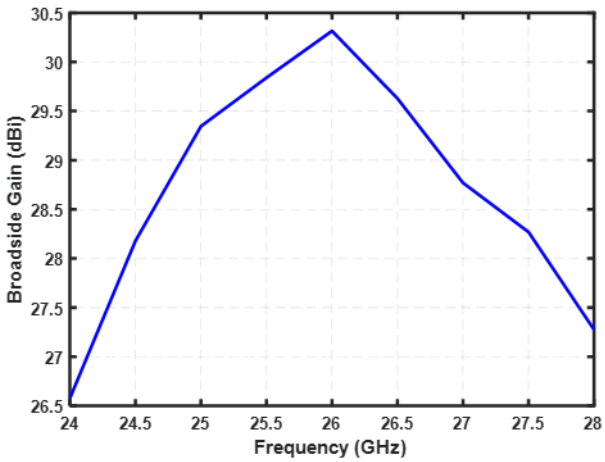


**FIGURE 21.** **Broadside gain of the prototype CP RLSA antenna on φ=0°**

TABLE VI
MEASURED PERFORMANCE OF FABRICATED PROTOTYPE AT 26 GHZ

| | Gain | Directivity | SLL | Angular Width 3-dB |
|---|---|---|---|---|
| | dBi | dBi | dB | (°) |
| phi=0° | 30.3 | 30.6 | -18 | 4.2 |
| phi=90° | 30.3 | 30.6 | -14 | 3.8 |

The measured performance values of the prototype antenna are summarized in Table VI. The radiation patterns of the simulated and prototype antennas are well matched at operating frequency. This proves the design methodology and confirms that non-uniform slot density can be used to improve pattern quality and aperture efficiency.



This work is licensed under a Creative Commons Attribution-NonCommercial-NoDerivatives 4.0 License. For more information, see https://creativecommons.org/licenses/by-nc-nd/4

This article has been accepted for publication in IEEE Access. This is the author's version which has not been fully edited and content may change prior to final publication. Citation information: DOI 10.1109/ACCESS.2023.3325193



### D. DISCUSSION

Summarized electrical and physical characteristics of the prototyped CP RLSA and previously published RLSA papers are given in Table VII. As it can be from the table that the proposed CP RLSA has the highest antenna aperture efficiency compared to the previously reported RLSAs. When the measured gain is compared, the prototype antenna has a better value than the large volume ones [16], [19], after the [30]. In addition, the measured gain value of the designed antenna is higher than both the same sized and smaller sized RLSA antennas [13], [14], [15], [17], [18]. The side lobe level of the new CP RLSA antenna has the second lower value after the [18].

Table VII lists the performance figures of some reflector antennas and compares them with prototyped CP RLSA. While, reflector antennas can exhibit high gain, they may also possess lower aperture efficiency [32]. Also, the proposed antenna has a better side lobe level and lower volume when compared to the ones whose efficiency is close to the prototyped CP RLSA [31], [33].

TABLE VII
COMPARING KEY PARAMETER OF THE PROPOSED CP RLSA WITH PREVIOUS DESIGN

| Ref. | Type | Frequency | Gain | Aperture Efficiency | Side Lobe Level | Axial Ratio | Diameter |
|---|---|---|---|---|---|---|---|
| | | GHz | dBi | % | dB | dB | mm |
| This Work (Measured) | RLSA | 26 | 30.3 | 45 | -18 | 1.2 | 180 |
| [13] (Sim.) | RLSA | 28 | 21.7 | 12 | -17 | - | 120 |
| [15] (Sim.) | RLSA | 28 | 20 | - | - | - | 130 |
| [17] (Sim.) | RLSA | 34.4 | 27 | 43 | -8 | 0.3 | 100 |
| [18] (Sim.) | RLSA | 11 | 22.1 | 40 | -20.8 | 0.7 | 180 |
| [14] (Meas.) | RLSA | 28 | 23.3 | 24.8 | -17.5 | - | 100 |
| [30] (Meas.) | RLSA | 12.5 | 31 | 24.6 | - | - | 550 |
| [16] (Meas.) | RLSA | 10.4 | 27.3 | 28.3 | -7.4 | <1 | 400 |
| [19] (Meas.) | RLSA | 9.42 | 29 | 28 | -9 | 1.12 | 540 |
| [31] | Reflector | 26.5-29.5 | 30 | - | - | - | 250 |
| [32] | Reflector | 28 | 48.5 | 25.4 | -24 | - | 1800 |
| [33] | Reflector | 28 | 32.1 | 47 | -13.6 | - | 200 |

## VI. CONCLUSION

This article presents an innovative design method for single-layered RLSA antennas with the aim of increasing aperture efficiency in part of the 5G FR2 bands. The new method offers significant advantages including high gain, high radiation efficiency, broadband impedance matching, and low SLLs. The results obtained from the prototype antenna verify its excellent performance. With the help of the new concept, the antenna aperture efficiency has reached 45%, which represents a performance improvement of 9% compared to the classical method. The antenna gain is measured 30.3 dB at 26 GHz and the antenna pattern matches well with the simulation results. Also, it has approximately 3.5 GHz 3 dB gain bandwidth from 24.5 GHz to 28 GHz. Measurement results have shown that the prototype has good pattern quality with an excellent side lobe level, which is less than -18 dB. In addition to some technical specifications, the antenna has a compact structure. The prototype antenna consists of only two metal parts made of aluminum and does not require any extra material such as dielectric, which brings eases the production process and ensures low loss. Also, since the use of aluminum results in lightness, these antennas can easily be used in aerial platforms.

## ACKNOWLEDGMENT

The authors are grateful to the Scientific and Technological Research Council of Turkey (TUBITAK) for supporting this study. We would also like to thank Dr. Daghan Dogan for their contributions in manufacturing.



This work is licensed under a Creative Commons Attribution-NonCommercial-NoDerivatives 4.0 License. For more information, see https://creativecommons.org/licenses/by-nc-nd/4

This article has been accepted for publication in IEEE Access. This is the author's version which has not been fully edited and
content may change prior to final publication. Citation information: DOI 10.1109/ACCESS.2023.3325193



## REFERENCES

[1] Huawei: '5g: A technology vision (white paper)', Huawei, 2013, Available https://www.huawei.com/mediafiles/CORPORATE/PDF/Magazine/WinWin/HW_329327.pdf

[2] Park, Y.: '5G vision and requirements of 5G forum'. Korea, 2014. Available at: https://www.itu.int/dms_pub/itu-r/oth/0a/06/R0A0600005F0001PDFE.pdf

[3] E. Strinati, M. Mueck, A. Clemente, J. Kim, G. Noh, H. Chung, I. Kim, T. Choi, Y. Kim, H. K. Chung, G. Destino, A. Parssinen, N. Chuberre, B. Vautherin, T. Deleu, M. Gineste, and A. Korvala, "5GCHAMPION – Disruptive 5G Technologies for Roll-Out in 2018," ETRI Journal, vol. 40, pp. 10–25, 02 2018.

[4] M. Kamal, S. Yang, S. Kiani, M. Anjum, M. Alibakhshikenari, Z. Arain, A. Jamali, and E. Limiti, "Donut-Shaped mmWave Printed Antenna Array for 5G Technology," Electronics, vol. 10, 06 2021.

[5] M. U. Afzal, N. Y. Koli and K. P. Esselle, "Low-Cost Radial Line Slot Array Antenna for Millimeter-Wave Backhaul Links," 2021 15th European Conference on Antennas and Propagation (EuCAP), Dusseldorf, Germany, 2021, pp. 1-4.

[6] A. Harmouch, K. Mawass, F. Shakra and C. El Mouccary, "Enhancement of directional characteristics of circularly polarized dish parabolic Antennas using metallic scatters," The 2nd Middle East Conference on Antennas and Propagation, Cairo, Egypt, 2012, pp. 1-5.

[7] P. Lam, Shung-Wu Lee, K. Lang and D. Chang, "Sidelobe reduction of a parabolic reflector with auxiliary reflectors," in IEEE Transactions on Antennas and Propagation, vol. 35, no. 12, pp. 1367-1374, December 1987.

[8] T. Purnamirza, "Radial line slot array (RLSA) antennas," in Telecommunication Systems, I. A. Alimi, P. P. Monteiro, and A. L. Teixeira, Eds. Rijeka, Croatia: IntechOpen, 2019, ch. 10.

[9] K. Kelly and F. Goebels, "Annular slot monopulse antenna arrays," in IEEE Transactions on Antennas and Propagation, vol. 12, no. 4, pp. 391-403, July 1964.

[10] M. Ando, K. Sakurai, N. Goto, K. Arimura and Y. Ito, "A radial line slot antenna for 12 GHz satellite TV reception," in IEEE Transactions on Antennas and Propagation, vol. 33, no. 12, pp. 1347-1353, December 1985.

[11] M. Ando, K. Sakurai and N. Goto, "Characteristics of a radial line slot antenna for 12 GHz band satellite TV reception," in IEEE Transactions on Antennas and Propagation, vol. 34, no. 10, pp. 1269-1272, October 1986.

[12] M. Ando, "New DBS receiver antennas," 1993 23rd European Microwave Conference, Madrid, Spain, 1993, pp. 84-92.

[13] R. Kamaruddin, I. Ibrahim, M. Rahim, Z. Zakaria, N. A. Shairi, and T. Rahman, "Radial Line Slot Array (RLSA) Antenna Design at 28 Ghz Using Air Gap Cavity Structure," J. Telecommun., Electron. Comput. Eng.,vol. 9, p. 2289, Oct. 2017.

[14] I. Maina, T. A. Rahman, and M. Khalily, "Bandwidth enhanced and sidelobes level reduced radial line slot array antenna at 28 GHz for 5G next generation mobile communication," ARPN J. Eng. Appl. Sci., vol. 10, pp. 5752–5757, Aug. 2015.

[15] H. Alwareth, I. Ibrahim, Z. Zakaria, A. Gburi, T. Purnamirza, M. H. Jamaluddin and L. Lau, "Enhanced Radial Line Slot Array Antenna (RLSA) integrated with Circular Ring Resonator (CRR) for 5G mm-wave applications," 2022 IEEE International RF and Microwave Conference (RFM), Kuala Lumpur, Malaysia, 2022, pp. 1-4.

[16] N. Y. Koli, M. U. Afzal, K. P. Esselle, "Significant Bandwidth Enhancement of Radial-Line Slot Array Antennas Using a Radially Nonuniform TEM Waveguide," IEEE Transactions on Antennas and Propagation, vol. 69, no. 6, pp. 3193–3203, June 2021.

[17] N. Y. Koli, M. U. Afzal, K. P. Esselle, L. Matekovits, and Z. Islam, "Highly Efficient and Wideband Millimeter-Wave Slotted-Array Antenna Technology for 5G Communications," 2022 16th European Conference on Antennas and Propagation (EuCAP), 2022, pp. 1–4.

[18] N. Y. Koli, M. U. Afzal, K. P. Esselle, L. Matekovits and Z. Islam, "Investigating Small Aperture Radial Line Slot Array Antennas for Medium Gain Communication Links," 2019 International Conference on Electromagnetics in Advanced Applications (ICEAA), Granada, Spain, 2019, pp. 0613-0616.

[19] C. -W. Yuan, S. -R. Peng, T. Shu, Z. -Q. Li and H. Wang, "Designs and Experiments of a Novel Radial Line Slot Antenna for High-Power Microwave Application," in IEEE Transactions on Antennas and Propagation, vol. 61, no. 10, pp. 4940-4946, Oct. 2013.

[20] T. Nguyen, K. Sakurai, J. Hirokawa, M. Ando, O. Amano, S. Koreeda, T. Matsuzaki, and Y. Kamata, "A concise design of large mm-Wave Radial Line Slot Antenna with honeycomb structures for space application," 2014 XXXIth URSI General Assembly and Scientific Symposium (URSI GASS), Beijing, China, 2014, pp. 1-4.

[21] J. M. Fernandez Gonzalez, P. Padilla, G. Exposito-Dominguez and M. Sierra-Castaner, "Lightweight Portable Planar Slot Array Antenna for Satellite Communications in X-Band," in IEEE Antennas and Wireless Propagation Letters, vol. 10, pp. 1409-1412, 2011.

[22] T. S. Lim and K. G. Tan, "The development of radial line slot array antenna for direct broadcast satellite reception," International Journal of Electronics, vol. 94, no. 3, pp. 251–261, Mar. 2007.

[23] M. N. Y. Koli, M. U. Afzal, K. P. Esselle and R. M. Hashmi, "An All-Metal High-Gain Radial-Line Slot-Array Antenna for Low-Cost Satellite Communication Systems," in IEEE Access, vol. 8, pp. 139422-139432, 2020.

[24] M. N. Y. Koli, M. U. Afzal, K. P. Esselle and R. M. Hashmi, "A Radial Line Slot-Array Antenna With Low Side Lobes and a Uniform-Phase, Tapered-Amplitude Aperture Field Distribution," in IEEE Access, vol. 8, pp. 208532-208542, 2020.

[25] M. N. Y. Koli, M. U. Afzal and K. P. Esselle, "Increasing the Gain of Beam-Tilted Circularly Polarized Radial Line Slot Array Antennas," in IEEE Transactions on Antennas and Propagation, vol. 70, no. 6, pp. 4392-4403, June 2022.

[26] M. Ando, T. Numata, J. . -I. Takada and N. Goto, "A linearly polarized radial line slot antenna," in IEEE Transactions on Antennas and Propagation, vol. 36, no. 12, pp. 1675-1680, Dec. 1988.

[27] P. W. Davis and M. E. Bialkowski, "Experimental investigations into a linearly polarized radial slot antenna for DBS TV in Australia," in IEEE Transactions on Antennas and Propagation, vol. 45, no. 7, pp. 1123-1129, July 1997.

[28] N. Y. Koli, M. U. Afzal, K. P. Esselle, R. M. Hashmi and M. Z. Islam, "A Low-profile and Efficient Front-End Antenna for Point-to-Point Wireless Communication Links," 2020 14th European Conference on Antennas and Propagation (EuCAP), Copenhagen, Denmark, 2020, pp. 1-4.

[29] M. E. Bialkowski, P. W. Davis, "Linearly polarized radial-line slot-array antenna with a broadened beam," Microwave and Optical Technology Letters, October 2000, 98-101.

[30] P. W. Davis and M. E. Bialkowski, "Linearly polarized radial-line slot-array antennas with improved return-loss performance," in IEEE Antennas and Propagation Magazine, vol. 41, no. 1, pp. 52-61, Feb. 1999.

[31] G. Mishra and S. K. Sharma, "Ka-Band Offset Spherical Reflector Antenna Fed by Dual-CP Horn Array with Switched Multiple-Beams," 2021 IEEE Radio and Wireless Symposium (RWS), San Diego, CA, USA, 2021, pp. 36-38.

[32] S. Chakrabarti, "A Shared Aperture S/Ka-Band Antenna for Polarization Diversity," 2018 IEEE Indian Conference on Antennas and Propagation (InCAP), Hyderabad, India, 2018, pp. 1-4.

[33] J. Wu, C. Wang and Y. X. Guo, "A Compact Reflector Antenna Fed by a Composite S/Ka-Band Feed for 5G Wireless Communications," in IEEE Transactions on Antennas and Propagation, vol. 68, no. 12, pp. 7813-7821.



This work is licensed under a Creative Commons Attribution-NonCommercial-NoDerivatives 4.0 License. For more information, see https://creativecommons.org/licenses/by-nc-nd/4

This article has been accepted for publication in IEEE Access. This is the author's version which has not been fully edited and content may change prior to final publication. Citation information: DOI 10.1109/ACCESS.2023.3325193





**ONUR CUMURCU** received the M.S degree in electronic and communication engineering from Yıldız Technical University, Istanbul, Turkey in 2017. He is currently pursuing the Ph.D. degree in communication engineering department, Yıldız Technical University and works a Senior Researcher at The Scientific and Technological Research Council of Turkey (TUBITAK). His research interests include high frequency circuits design, receiver and oscillator systems, millimeter wave antennas, radar systems and computer-aided circuit design.



**HAMID TORPI** received his B.S. degree in electronics and communication engineering and the M.S. degree, both from Yıldız University, Istanbul, Turkey, in 1988 and 1991, respectively, and the Ph.D. degree from Yıldız Technical University (YTU) in 1997. He is currently an Associated. Professor at YTU. His research interests include neural network applications of microwave circuit and devices, antennas, and design of microwave circuits and devices. Dr. Torpi is a recipient of science awards from Turkish Scientific and Technical Research Council and YTU.

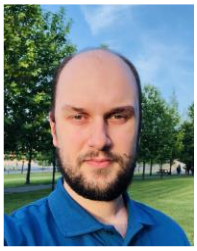

**ALPER CALISKAN** received the M.S. and Ph.D. degrees in electronics and communication engineering from Yıldız Technical University, in 2014 and 2019, respectively. From 2013 to 2021, he was a Research Assistant with the electronics and communication engineering. He is currently an Assistant Professor with the Department of Electronics and Communication Engineering Department, Yıldız Technical University. His main research interests include the optimization of microwave and millimeter wave antennas, development of ultra-wideband antennas, fabrication of 3D printed antennas, ground penetrating radar systems, and computer-aided circuit design.



This work is licensed under a Creative Commons Attribution-NonCommercial-NoDerivatives 4.0 License. For more information, see https://creativecommons.org/licenses/by-nc-nd/4